

Neural Machine Translation Inspired Binary Code Similarity Comparison *beyond Function Pairs*

Fei Zuo*, Xiaopeng Li*, Zhexin Zhang*, Patrick Young†, Lannan Luo*, Qiang Zeng*

* Department of Computer Science and Engineering, University of South Carolina, Columbia, SC 29208, USA

†Department of Computer and Information Sciences, Temple University, Philadelphia, PA 19122, USA

Email: {fzuo, xl4, zhexin}@email.sc.edu, tua43500@temple.edu, {lluo, zeng1}@cse.sc.edu

Abstract—**Binary code analysis allows analyzing binary code without having access to the corresponding source code.** A binary, after disassembly, is expressed in an *assembly language*. This inspires us to approach binary analysis by leveraging ideas and techniques from *Natural Language Processing* (NLP), a rich area focused on processing text of various natural languages. We notice that binary code analysis and NLP share a lot of analogical topics, such as *semantics extraction*, *summarization*, and *classification*. This work utilizes these ideas to address two important code similarity comparison problems. (I) Given a pair of basic blocks for different instruction set architectures (ISAs), determining whether their semantics is similar or not; and (II) given a piece of code of interest, determining if it is contained in another piece of assembly code for a different ISA. The solutions to these two problems have many applications, such as cross-architecture vulnerability discovery and code plagiarism detection.

Despite the evident importance of Problem I, existing solutions are either inefficient or imprecise. Inspired by Neural Machine Translation (NMT), which is a new approach that tackles text across natural languages very well, we regard *instructions as words and basic blocks as sentences*, and propose a novel *cross-(assembly)-lingual* deep learning approach to solving the first problem, attaining high efficiency and precision. Regarding Problem II, many solutions have been proposed recently to solve this issue at the function level. However, performing cross-architecture code similarity comparison *beyond function pairs* is a *new* and more challenging endeavor. Employing our technique for cross-architecture basic-block comparison, we propose the first solution to Problem II. We implement a prototype system INNEREYE and perform a comprehensive evaluation. A comparison between our approach and existing approaches to Problem I shows that our system outperforms them in terms of accuracy, efficiency and scalability. And the case studies utilizing the system demonstrate that our solution to Problem II is effective. Moreover, this research showcases how to apply ideas and techniques from NLP to large-scale binary code analysis.

I. INTRODUCTION

Binary code analysis allows one to analyze binary code without access to the corresponding source code. It is widely used for vulnerability discovery, code clone detection, user-side crash analysis, etc. Today, binary code analysis has become more important than ever. Gartner forecasts that 8.4 billion IoT devices will be in use worldwide in 2017, up 31 percent from 2016, and will reach 20.4 billion by 2020 [21]. Due to code reuse and sharing, a single vulnerability at source code level may spread across hundreds or more devices that have diverse hardware architectures and software platforms [50]. However, it is difficult, often unlikely, to obtain the source code from the many IoT device companies. Then, binary code analysis becomes the only feasible approach.

Recently, one binary code analysis problem has drawn great interests [50], [17], [18], [66]. Given a code component, such as a function, that is known to contain some vulnerability, and a large number of programs that are compiled for different ISAs, by finding programs that contain similar code components, more instances of the vulnerability can be found.

Our insight. A binary, after disassembly, is represented in some *assembly language*. This inspires us to approach binary code analysis by learning from Natural Language Processing (NLP), a fruitful area focused on processing natural language corpora effectively and efficiently. Interestingly, the two seemingly remote areas—binary code analysis and NLP—actually share plenty of analogical topics, such as *semantics extraction from code/text*, *summarization of paragraphs/functions*, *classification of code/articles*, and *code/text similarity comparison*. We thus propose to apply the ideas, methods, and techniques used in NLP to resolving binary code analysis problems. As showcases, we utilize the idea to resolve the aforementioned *cross-architecture binary code similarity comparison* problem.

But unlike previous work [50], [17], [18], [66] on this problem that assumes the code component of interest is always a function, our system considers a code component that is much more flexible: it can be part of a function (e.g., the code in a web server that parses the URL), or a set of functions (e.g., an implementation of a crypto algorithm). Such a system certainly provides a useful and important capability, i.e., code similarity comparison beyond function pairs, which has been emphasized by previous work [27], [37], [43], [68], [26], [60], [61] (, although they can only work for code of the same ISA). In addition to supporting more capable vulnerability search, the capability is critical for fine-grained code plagiarism detection, as the plagiarist may copy the code from part of a function or a bunch of functions, and then insert the stolen code to the original code; that is, the stolen code is not necessarily a function. Code plagiarism detection at the function level is too limited to handle such cases.

We thus define two research problems concerning cross-architecture code similarity comparison: (I) given a pair of binary basic blocks for different instruction set architectures (ISAs), determining whether their semantics is similar or not; and (II) given a piece of critical code, determining if it is contained in another piece of code of a different ISA. Problem I is one of the *core* sub-problems in all the recent work on cross-architecture similarity comparison [50], [17], [18], [66], while Problem II is new.

Solution to Problem I. Problem I is one of the most

fundamental problems for code comparison; therefore, many approaches have been proposed to resolve it, such as fuzzing [50] and representing a basic block using some features [17], [18], [66]. However, none of existing approaches are able to achieve both high efficiency and precision for this important problem. Fuzzing takes much time to try different inputs, while the feature-based representation is imprecise (A SVM classifier based such features can only achieve $AUC = 85\%$ according to our evaluation). Given a pair of blocks of different architectures, they, after being disassembled, are two sequences of instructions in two different assembly languages. In light of this insight, we propose to learn from the ideas and techniques of Neural Machine Translation (NMT), a new machine translation framework based on neural networks proposed by NLP researchers that handles text *across* languages very well [30], [55]. NMT frequently uses Recurrent Neural Network (RNN) with Long Short-Term Memory (LSTM), which is capable of *learning features and dependencies between words in a sentence and encoding the sentence into a vector representation that captures its semantic meaning* [48], [46], [64]. In addition to translating sentences, the NMT model has also been extend to measure the similarity of sentences by comparing their vector representations [46], [48].

We regard *instructions as words and basic blocks as sentences* during binary code analysis, and consider that the task of *detecting whether two basic blocks of different ISAs are semantically similar* is analogous to *that of determining whether two sentences of different human languages have similar meanings*. Following this idea and learning from NMT, we propose a novel neural network-based *cross-(assembly)-lingual basic-block embedding model*, which converts a basic block into an *embedding*, i.e., a high dimensional numerical vector. The embeddings not only encode basic-block semantics, but also capture semantic relationships across architectures, such that the similarity of two basic blocks can be detected efficiently by measuring the distance between their embeddings.

Recent work [17], [18], [66] uses several *manually* selected features (such as the number of instructions and constants) of a basic block to represent it. This inevitably causes significant loss of information, for example, which instructions are used and the dependencies between these instructions. In contrast to using manually selected features, our NMT-inspired approach applies deep learning to *automatically* encoding the information of basic blocks. Specifically, we propose to employ LSTM-RNN to automatically (i.e., no need to manually select features) encode a basic block into an embedding that captures the semantic information of the instruction sequence, just like LSTM-RNN is used in NMT to capture the semantic information of sentences. This way, our cross-(assembly)-lingual deep learning approach to Problem I achieves both high efficiency and precision.

Gemini [66] also applies neural networks. There are two main differences between our systems and theirs. First, Gemini uses *manually* selected features to represent a basic block. Second, it encodes the CFG of a function into an embedding and can only handle function-level comparison.

Solution to Problem II. A variant of Problem II is well studied under the context of a single architecture [32], [29], [2], [59], [67], [28], [52], [51], [20], [37], [56], [53], [60], [27]; but they can only handle code of the *same* architecture. Many systems have been proposed recently to compare *functions*

of different architectures [50], [17], [18], [66]. To perform cross-architecture code similarity comparison *beyond function pairs*, we decompose the control flow graph (CFG) of the code of interest into multiple paths, each of which can be regarded as *a sequence of basic blocks*. Our idea is to leverage our solution to Problem I for efficient and precise basic-block comparison when applying the *Longest Common Subsequence* (LCS) algorithm to comparing the similarity of those paths (i.e., basic-block sequences). From there, we can calculate the similarity of two pieces of code quantitatively.

Note that *we do not simply consider functions to be sentences*, because a function cannot be treated as a straight-line sequence. When a function is invoked, its code is not executed sequentially; instead, only a part of the code belonging to a particular *path* gets executed, while the code for the semantically equivalent two paths in two functions may be placed into very different positions.

We have implemented a prototype system INNEREYE consisting of two components: INNEREYE-BB for cross-architecture basic-block similarity comparison and INNEREYE-CC for cross-architecture code-component similarity comparison. We have evaluated INNEREYE-BB in terms of accuracy, efficiency and scalability, and the evaluation results show that it outperforms existing approaches by large margins. Our case studies utilizing INNEREYE-CC demonstrate that it can successfully resolve cross-architecture code similarity comparison tasks and is much more capable than recent work that is limited to comparison of function pairs. The trained NN models, datasets, and evaluation results are publicly available.¹

We summarize our contributions as follows:

- We propose to learn from the successful NMT field to solve the cross-architecture binary code similarity detection problem. *We regard instructions as words and basic blocks as sentences*. Thus, the ideas and methodologies for comparing the meanings of sentences in different natural languages can be adapted to comparing cross-architecture code similarity.
- We design a precise and efficient cross-(assembly)-lingual basic block embedding model. It utilizes LSTM-RNN, a neural network structure frequently used in NMT, to automatically capture the semantics information of the instruction sequence. This is in contrast to prior work which ignores such information and relies on manually selected features.
- We propose the *first* system that can handle cross-architecture code similarity comparison *that is not limited to function pair comparison*. It can have many applications, such as code plagiarism detection and malware identification.
- We implement a prototype INNEREYE and evaluate its accuracy, efficiency, and scalability. We use real-world software across various architectures to demonstrate the applications of INNEREYE for cross-architecture binary code similarity detection.
- This research successfully demonstrates that it is promising to approach binary analysis from the angle

¹<https://nmt4binaries.github.io>

of language processing by adapting methodologies, ideas and techniques in NLP.

II. RELATED WORK

The related work can be divided into two classes: traditional and machine learning based. Each class can be divided into two categories: mono-architecture and cross-architecture based.

A. Traditional Code Similarity Detection

Mono-architecture based. Most traditional code analysis approaches, including control flow analysis, data flow analysis, symbolic execution, and trace analysis, work under the context of a *single* architecture. First, static plagiarism detection or clone detection includes string-based [2], [6], [16], AST-based [29], [59], [33], token-based [32], [28], [52], [51], and PDG-based [19], [36], [15], [35]. Some approaches are *source code based*, and are less applicable in practice, especially concerning closed-source software; e.g., CCFINDER [32] finds equal suffix chains of source code tokens. DECKARD [29] leverages abstract syntax trees and local sensitive hashes to find similar subtrees of source code. Others compare the semantics of binary code using symbolic execution and theorem prover, such as BinHunt [20] and CoP [37], but are *computation expensive*, and thus are not applicable for large codebases.

Second, dynamic birthmark based approaches include API birthmark [56], [53], [57], [8], system call birthmark [60], function call birthmark [56], instruction birthmark [58], [49], and core-value birthmark [27]. Tamada et al. propose an API birthmark for Windows application [56]. Schuler et al. propose a dynamic birthmark for Java [53]. Wang et al. introduce two system call based birthmarks suitable for programs invoking sufficient system calls [60]. Jhi et al. propose a core-value based birthmark for detecting plagiarism [27], [26]. However, as they rely on dynamic analysis, *extending them to other architectures and adapting to embedded devices would be hard and tedious*.

Cross-architecture based. Recently, researchers have started to address the problem of cross-architecture binary code similarity detection. Multi-MH and Multi-k-MH [50] are the first two methods for comparing *function* code across different architectures. However, their fuzzing-based basic block similarity comparison and graph (i.e., CFG) matching-based algorithm are too expensive to handle millions of graph pairs. discovRE [17] utilizes pre-filtering to boost *CFG* based matching process, but it is still expensive, and the pre-filtering is unreliable, outputting too many false negatives.

B. Machine Learning-based Code Similarity Detection

Mono-architecture based. Recent research has demonstrated the usefulness of applying machine learning and deep learning techniques to code analysis [44], [38], [45], [25], [63], [24], [34], [47], [22]. White et al. further propose DeepRepair to detect the similarity between *source code* fragments [63]. Mou et al. propose a tree-based convolutional neural network based on program abstract syntax trees to detect similar *source code* snippets [45]. Huo et al. propose NP-CNN [25] and LS-CNN [24] to identify buggy *source code* files. Zheng et al. [12] independently proposed to use word embedding to represent instructions, but their word-embedding model does not address the issue of out-of-vocabulary (OOV) instructions,

while handling OOV words has been a critical step in NLP that is resolved in our system (Section IV-C); plus, their goal is to recover function signature from binaries of the same architecture, which is different from our cross-architecture code similarity comparison task. Nguyen et al. propose API2VEC for the API elements in *source code* to measure code similarity [47], which is not applicable if there are insufficient API calls.

Cross-architecture based. Genius [18] and Gemini [66] are the two current state-of-the-art works on cross-architecture bug search. They make use of conventional machine learning and deep learning, respectively, to convert CFGs of *functions* into vectors for similarity comparison. BinGo [9] proposes a selective inlining technique to capture the function semantics and extracts length variant partial traces to model functions. But all three of these approaches compare similarity between functions, and cannot handle code component similarity detection when only a *part* of a function or code cross function boundaries is reused in another program.

Summary. Currently, no work is able to meet all these requirements: (a) directly working on binary code, (b) analyzing code of *different architectures*, (c) measuring code similarity *beyond function pairs*, and (d) comparing code similarity efficiently. This work aims to fill the gap and proposes techniques for efficient cross-architecture binary code similarity comparison beyond function pairs. In addition, it is worth mentioning that many prior systems are built on basic block comparison or representation [20], [42], [37], [50], [18]; thus, *they can benefit from our system, which provides more precise and efficient basic block comparison and information extraction*.

III. OVERVIEW

Given a *query* binary code component Q , consisting of basic blocks whose relation can be represented in a control flow graph (CFG), we are interested in detecting a list of code components from a large corpus of binary programs, compiled for different architectures (e.g., x86 and ARM), that are semantically equivalent or similar to Q . A code component here can be a *part* of a function or multiple functions.

We extract code component semantics at three layers: basic blocks, CFG paths, and code components. The system architecture is shown in Figure 1. The inputs are the query code component and a set of target programs. The *front-end* disassembles each binary and constructs its control-flow graph. (1) To model the semantics of a basic block, we design the *neural network-based cross-lingual basic-block embedding model* to represent a basic block as an embedding. The embeddings of all blocks are stored in a locality-sensitive hashing (LSH) database for efficient online search. (2) The *path similarity comparison* component utilizes the Longest Common Subsequence (LCS) algorithm to compare the semantic similarity of two paths, one from the query code component and another from the target program, constructed based on the LCS dynamic programming algorithm with basic blocks as the sequence elements. The length of this common subsequence is then compared to the length of the path from the query code component. The ratio indicates the semantics of the query path as embedded in the target program. (3) The *component similarity comparison* component explores multiple path pairs to collectively calculate a similarity score, indicating the likelihood of the query code component being reused in the target program.

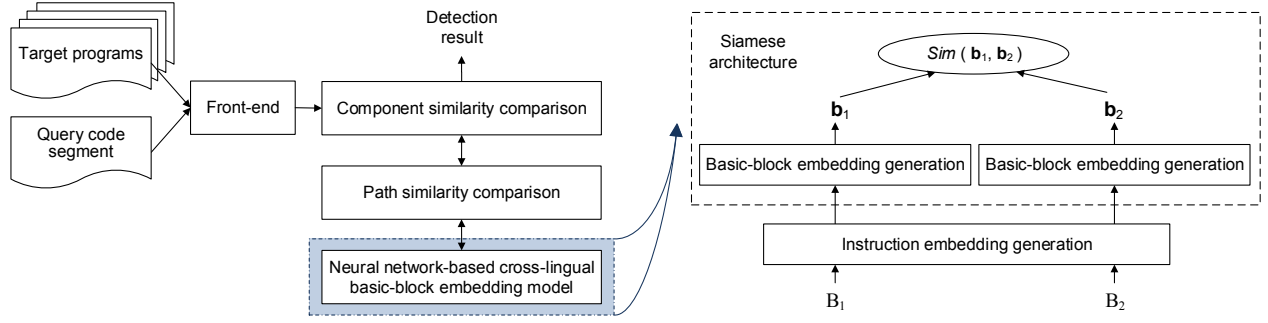


Fig. 1: System architecture.

Basic Block Similarity Detection. The key is to measure the similarity of two blocks, *regardless of their target ISAs*. As shown in the right side of Figure 1, the neural network-based cross-lingual basic-block embedding model takes a pair of blocks as inputs, and computes a similarity score $s \in [0, 1]$ as the output. The objective is that the more the two blocks are similar, the closer s is to 1, and the more the two blocks are dissimilar, the closer s is to 0. To achieve this, the model adopts a Siamese architecture [7] with each side employing the LSTM-RNN [23]. The Siamese architecture is a popular network architecture among tasks that involve finding similarity between two comparable things [7], [11]. The LSTM-RNN is capable of learning long range dependencies of a sequence. The two LSTM-RNNs are trained *jointly* to tolerate the cross-architecture syntactic variations.

The block embedding model converts each block into a vector representation. Such a vector representation is called an *embedding*. Specifically, if a vector is to represent a basic block, we call it a *block embedding*. Similarly, a vector that represents an instruction is called an *instruction embedding*.

Three main steps are involved to detect the similarity of two blocks, as shown in the right side of Figure 1. (1) Instruction embedding generation: given a block, each of its instructions is converted into an *instruction embedding* using an instruction embedding matrix, which is learned via a neural network (Section IV). (2) Basic-block embedding generation: the first step essentially extracts semantic features of a block. These features are then fed into a neural network to generate the *block embedding* (Section V). (3) Once the embeddings of two blocks have been obtained, their similarity can be detected efficiently by measuring the distance between their block embeddings.

A prominent advantage of the model inherited from Neural Machine Translation, is that it does not need to select features *manually* when training the models; instead, as we will show later, the models *automatically* select useful features during the training process. In contrast, the state-of-the-art Genius [18] and Gemini [66] need to *manually* select the basic-block features and cannot capture the semantics information of the instruction sequence within a block. As a result, the precision of our approach outperforms theirs by large margin. This is shown in our evaluation (Section VII-E3).

IV. INSTRUCTION EMBEDDING GENERATION

An instruction includes an opcode (specifying the operation to be performed) and zero or more operands (specifying

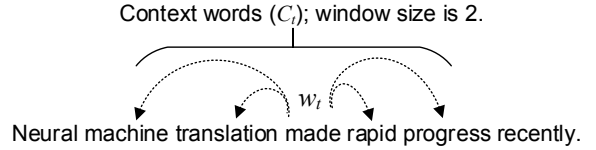


Fig. 2: A sliding window used in Skip-gram.

registers, memory locations, or literal data). For example, `mov eax, ebx` is an instruction where `mov` is an opcode and both `eax` and `ebx` are operands. In NMT, words are usually converted into word embeddings to facilitate further processing. As we regard instructions as words, similarly we propose to represent instructions into *instruction embeddings*.

Our notations use blackboard bold upper case to denote functions (e.g., \mathbb{F}), capital letters to denote basic blocks (e.g., B), bold upper case to represent matrices (e.g., \mathbf{U} , \mathbf{W}), bold lower case to represent vectors (e.g., \mathbf{x} , \mathbf{y}_i), and lower case to represent individual instructions in a basic block (e.g., x_1 , y_2).

A. Background: Word Embedding

A unique aspect of Neural Machine Translation (NMT) is its heavy use of embeddings, which are high-dimensional numerical vectors, to represent words to facilitate the further processing in neural networks. Specifically, a word embedding is to capture the contextual semantic meaning of the word; thus, words that have similar contexts have embeddings that are close in the high-dimensional space. Recently, a series of models [40], [41], [5] applying deep learning techniques have been proposed to learn high-quality word embeddings. Among these models, Mikolov’s *skip-gram* model is popular due to its efficiency and low memory usage relative to other models [40].

The skip-gram model learns word embeddings by using a neural network. During training, a sliding window is employed on a text stream. In Figure 2, for example, a window of size 2 is used, covering two words behind the current word and two words ahead. The model starts with a random vector for each word, and then gets trained when going over each sliding window. In each sliding window, the embedding of the current word, \mathbf{w}_t , is used as the parameter vector of a *softmax* function (Equation 1) that takes an arbitrary word w_k as a training input and is trained to predict a probability of 1, if w_k appears in the context C_t (i.e., the sliding window) of w_t , and 0, otherwise.

$$P(w_k \in C_t | w_t) = \frac{\exp(\mathbf{w}_t^T \mathbf{w}_k)}{\sum_{w_i \in C_t} \exp(\mathbf{w}_t^T \mathbf{w}_i)} \quad (1)$$

where \mathbf{w}_k , \mathbf{w}_t , and \mathbf{w}_i are the embeddings of words w_k , w_t , and w_i , respectively.

Thus, given an arbitrary word w_k , its vector representation \mathbf{w}_k is used as a feature vector in the *softmax* function parameterized by \mathbf{w}_t . When trained on a sequence of T words, the model uses stochastic gradient descent to maximize the log-likelihood objective $J(\mathbf{w})$ as showed in Equation 2.

$$J(\mathbf{w}) = \frac{1}{T} \sum_{t=1}^T \sum_{w_k \in C_t} (\log P(w_k|w_t)) \quad (2)$$

However, it would be very expensive to maximize $J(\mathbf{w})$, because the denominator $\sum_{w_i \in C_t} \exp(\mathbf{w}_t^T \mathbf{w}_i)$ sums over all words w_i in C_t . To minimize the computational cost, popular solutions are negative sampling and hierarchical softmax. We adopt the *skip-gram with negative sampling model* (SGNS) [41]. After the model is trained on many sliding windows, the embeddings of each word become meaningful, yielding similar vectors for similar words. Due to its simple architecture and the use of the hierarchical softmax, the skip-gram model can be trained on a desktop machine at billions of words per hour. Plus, learning the word embedding is entirely *unsupervised*.

B. Challenges

Some unique challenges arise when learning instruction embeddings. First, in NMT, words are usually represented into vectors using a word embedding model, which is trained once using large corpora, such as *Wiki*, and then ready to be used by other researchers [65]. However, we have to *train an instruction embedding model from scratch*.

Second, if a trained model is used to convert a word that has never appeared during training, the word is called an *out-of-vocabulary* (OOV) word and the embedding generation for such words will fail. This is a well-known problem in NLP, and it exacerbates significantly in our case, as constants, address offsets, labels, and strings are frequently used in instructions. How to deal with the OOV problem is a challenge.

C. Building Training Dataset

Because we regard blocks as sentences, we use instructions of each block, called a *Block-level Instruction Stream* (BIS) (Definition 1), to train the instruction embedding model.

Definition 1: (Block-level Instruction Stream) Given a basic block B , consisting of a list of instructions. The *block-level instruction stream* (BIS) of B , denoted as $\pi(B)$, is defined as

$$\pi(B) = (b_1, \dots, b_n)$$

where b_i is an instruction in B .

Preprocessing Training Data. To resolve the OOV problem, we propose to preprocess the instructions in the training dataset using the following rules: (1) The number constant values are replaced with 0, and the minus signs are preserved. (2) The string literals are replaced with `<STR>`. (3) The function names are replaced with `FOO`. (4) Other symbol constants are replaced with `<TAG>`. Take the following code snippets as an example: the left code snippet shows the original assembly code, and the right one is the preprocessed result.

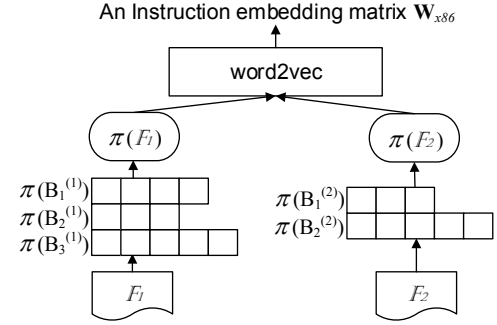


Fig. 3: Learning instruction embeddings for x86. $\pi(B_i^{(j)})$ represent the i -th block-level instruction stream (BIS) in the function \mathbb{F}_j . Each square in a BIS represents an instruction.

```
MOVL %ESI, $.L.STR.31
MOVL %EDX, $3
MOVQ %RDI, %RAX
CALLQ STRNCMP
TESTL %EAX, %EAX
JE .LBB0_5
```

```
MOVL ESI, <STR>
MOVL EDX, 0
MOVQ RDI, RAX
CALLQ FOO
TESTL EAX, EAX
JE <TAG>
```

Note that the same preprocessing rules are applied to instructions before generating their embeddings. This way, we can significantly reduce the OOV cases. Our evaluation result (Section VII-C) shows that, after a large number of preprocessed instructions are collected to train the model, we encounter very few OOV cases in the later testing phase. This means that the trained model is readily *reusable* for other researchers. Moreover, semantically similar instructions do indeed have embeddings that are close to each other, as predicted.

D. Training Instruction Embedding Model

We adapt the skip-gram word embedding model `word2vec` [40], a two-layer neural network, to obtain our instruction embedding model. As an example, Figure 3 shows the process of training the model for the x86 architecture. Given an architecture, the model is trained using the functions in our dataset built from many binaries; each function is parsed to generate the corresponding Block-level Instruction Streams (BISs), which are fed, BIS by BIS, into the model for training. The training result is an instruction embedding matrix containing the instruction embedding for each instruction.

The training result is an instruction embedding matrix $\mathbf{W} \in \mathbf{R}^{d^e \times V}$, where d^e is the dimensionality of the instruction embedding selected by users (how to select d^e is discussed in Section VII-F) and V the number of distinct instructions in the vocabulary. Each column $\mathbf{W}_i \in \mathbf{R}^{d^e}$ corresponds to the instruction embedding for the i -th instruction in the vocabulary (all distinct instructions form a vocabulary).

Embedding Generation. The embedding of an instruction i is generated as a matrix-vector product:

$$\mathbf{e}_i = \mathbf{W}\mathbf{u}^i \quad (3)$$

where \mathbf{u}^i is a $V \times 1$ vector, which has the value *one* at the index i (and zeros at others).

Source code	
<pre>numblocks = (tmp_len+blocksize-1)/blocksize; if(numblocks > pre_comp->numblocks)</pre>	
<i>X86-64 assembly</i>	<i>ARM assembly</i>
<pre>movq %rsi,80(%rsp) addq %rax,%rsi addq %rax,\$-1 xorl %edx,%edx divq %rsi movq %rdx,96(%rsp) cmpq %rax,16(%rdx) jbe .LBB2_68</pre>	<pre>adds r1, r2, r1 adc r7, r3, r0 subs r0, r1, #1 sbc r1, r7, #0 bl __udivdi3 ldr r3, [sp, #60] ldr r2, [r3, #16] ldr r3, [r3, #20] subs r2, r2, r0 sbc r2, r3, r1 bhs .LBB2_120</pre>

Fig. 4: C source of a basic block from `ec_mult.c` in OpenSSL and the assembly code for two architectures.

V. BLOCK EMBEDDING GENERATION

A. Design Choice

A straightforward attempt for generating the embedding of a basic block is to simply compose (e.g., summing up) all embeddings of the instruction in the basic block. However, this processing cannot handle the cross-architecture differences, as instructions that stem from the same source code but target different architectures may have very different embeddings. This is verified in our evaluation (Section VII-D).

Take Figure 4 as an example. It shows a small code snippet (containing one basic block) that has been compiled for two different architectures, x86 and ARM. Although the two binaries stem from the same source code, they are very different due to various instruction sets, general- and special-purpose CPU register usages, and memory access strategies.

As a trivial example, the following two *load* byte instructions (1) `lodsb` and (2) `ldrb r3 [r1]` are compiled on x86 and ARM, respectively; they are similar in semantics. However, our instruction embedding model generates *distant* instruction embeddings for them, as the model has no way to learn these instructions are semantically similar. Therefore, such a naive comparison of instruction embeddings cannot measure the similarity of instructions across-architectures.

B. Background: LSTM-RNN in NLP

The recurrent neural network (RNN) is a type of deep neural network that has been successfully applied to converting word embeddings of a sentence to a sentence embedding [13], [14], [31]. LSTM-RNN is a specific RNN, developed to address the difficulty of capturing long term memory in the basic RNN. A reasonable limit of 500 words is often used in practice, and a basic block usually contains less than 500 instructions.

In text analysis, LSTM-RNN treats a sentence as a sequence of words with internal structures, i.e., word dependencies or relations. It encodes the semantic vector of a sentence incrementally. The encoding process is performed left-to-right, word-by-word. At each time step, a new word is encoded and the word dependencies embedded in the vector are “updated”. When the process reaches the end of the sentence, the semantic vector has embedded all the words and their dependencies, and

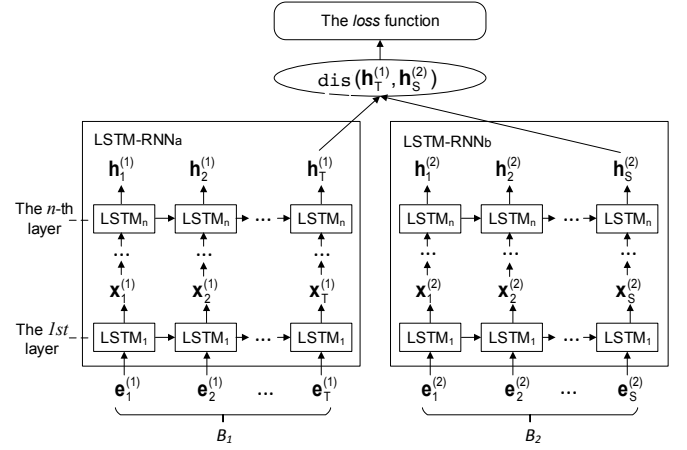


Fig. 5: Neural network-based basic-block embedding model.

hence, can be viewed as a feature representation of the whole sentence. The final semantic vector is the sentence embedding.

C. Cross-lingual Basic-block Embedding Model Architecture

Inspired by the NMT model that compares the similarity of sentences of different languages, we design a *neural network-based cross-lingual basic-block embedding model* to compare the semantics similarity of basic blocks of different ISAs. As showed in Figure 5, we design our model as a *Siamese architecture* [7] with each side employing the *identical* Recurrent Neural Network (RNN) with Long Short-Term Memory (LSTM). Our objective is to *make the embeddings for blocks of similar semantics as close as possible, and meanwhile, to make blocks of different semantics as far apart as possible*. A Siamese architecture takes the embeddings of instructions in two blocks, B_1 and B_2 , as inputs, and produces the similarity score as an output. This model is trained with only supervision on a basic-block pair as input and the ground truth $\chi(B_1, B_2)$ as an output *without relying on any manually selected features*.

For embedding generation, each LSTM cell sequentially takes an input (for the first layer the input is an instruction embedding) at each time step, accumulating and passing increasingly richer information. When the last instruction embedding is reached, the last LSTM cell at the last layer provides a semantic representation of the basic block, i.e., a block embedding. Finally, the similarity of the two basic blocks is measured as the distance of the two block embeddings.

Detailed Process. The inputs are two blocks, B_1 and B_2 , represented as a sequence of instruction embeddings, $(\mathbf{e}_1^{(1)}, \dots, \mathbf{e}_T^{(1)})$, and $(\mathbf{e}_1^{(2)}, \dots, \mathbf{e}_S^{(2)})$, respectively. Note that the sequences may be of different lengths, i.e., $|T| \neq |S|$, and the sequence lengths can vary from example to example; both are handled by the model. LSTM-RNN updates its hidden state at each time step and at each time step an LSTM cell analyzes an input vector coming from either the input embeddings or the precedent step. Each memory cell contains four components (which are real-valued vectors): a *memory state* c , an *output gate* o determining how the memory state affects other units, and an *input gate* i (and a *forget gate* f , resp.) that controls what gets stored in (and omitted from, resp.) memory. For example, an LSTM at the first layer in LSTM-RNN_a updates

its hidden state at the time step t via Equations 4–9:

$$\mathbf{i}_t^{(1)} = \text{sigmoid}(\mathbf{W}_i \mathbf{e}_t^{(1)} + \mathbf{U}_i \mathbf{x}_{t-1}^{(1)} + \mathbf{v}_i) \quad (4)$$

$$\mathbf{f}_t^{(1)} = \text{sigmoid}(\mathbf{W}_f \mathbf{e}_t^{(1)} + \mathbf{U}_f \mathbf{x}_{t-1}^{(1)} + \mathbf{v}_f) \quad (5)$$

$$\tilde{\mathbf{c}}_t^{(1)} = \tanh(\mathbf{W}_c \mathbf{e}_t^{(1)} + \mathbf{U}_c \mathbf{x}_{t-1}^{(1)} + \mathbf{v}_c) \quad (6)$$

$$\mathbf{c}_t^{(1)} = \mathbf{i}_t^{(1)} \odot \tilde{\mathbf{c}}_t^{(1)} + \mathbf{f}_t^{(1)} \odot \tilde{\mathbf{c}}_t^{(1)} \quad (7)$$

$$\mathbf{o}_t^{(1)} = \text{sigmoid}(\mathbf{W}_o \mathbf{e}_t^{(1)} + \mathbf{U}_o \mathbf{x}_{t-1}^{(1)} + \mathbf{v}_o) \quad (8)$$

$$\mathbf{x}_t^{(1)} = \mathbf{o}_t^{(1)} \odot \tanh(\mathbf{c}_t^{(1)}) \quad (9)$$

where \odot denotes Hadamard (element-wise) product; $\mathbf{W}_i, \mathbf{W}_f, \mathbf{W}_c, \mathbf{W}_o, \mathbf{U}_i, \mathbf{U}_f, \mathbf{U}_c, \mathbf{U}_o$ are weight matrices; and $\mathbf{v}_i, \mathbf{v}_f, \mathbf{v}_c, \mathbf{v}_o$ are bias vectors; they are learned during training. The reader is referred to [23] for more details.

At the last time step T , the last hidden state at the last layer provides a vector $\mathbf{h}_T^{(1)}$ (resp. $\mathbf{h}_S^{(1)}$), which is the embedding of B_1 (resp. B_2). We use the Manhattan distance ($\in [0, 1]$) to measure the similarity of B_1 and B_2 as showed in Equation 10:

$$\text{Sim}(B_1, B_2) = \exp(-\|\mathbf{h}_T^{(1)} - \mathbf{h}_S^{(1)}\|_1) \quad (10)$$

To train the network parameters, we use stochastic gradient descent (SGD) to minimize the *loss* function:

$$\min_{\mathbf{W}_i, \mathbf{W}_f, \dots, \mathbf{v}_o} \sum_{i=1}^N (y_i - \text{Sim}(B_1^i, B_2^i))^2 \quad (11)$$

where y_i is the similarity ground truth of the pair $\langle B_1^i, B_2^i \rangle$, and N the number of basic block pairs in the training dataset.

In the end, once the Area Under the Curve (AUC) value converges, the training process terminates, and the trained cross-lingual basic-block embedding model is capable of encoding an input binary block to an embedding capturing the semantics information of the block that is suitable for similarity detection.

D. Challenges

There are two main challenges for learning block embeddings. First, in order to train, validate and test the basic-block embedding model, a large dataset containing labeled similar and dissimilar block pairs is needed. Unlike prior work [66] that builds the dataset of similar and dissimilar *function* pairs by using the function names to establish the ground truth about the *function* similarity, it is very challenging to establish the ground truth for basic blocks because: (a) no name is available to indicate whether two basic blocks are similar or not, and (b) even if two basic blocks have been compiled from two *different* pieces of code, they may happen to be equivalent, and therefore, it would be incorrect to label them as dissimilar.

Second, many hyperparameters need to be determined to maximize the model performance. The parameter values selected for NMT are not necessarily applicable to our model, and need to be comprehensively examined.

E. Building Dataset

1) *Generating Similar Basic-Block Pairs*: We consider two basic blocks of different ISAs that have been compiled from the same piece of source code as equivalent. To establish the ground truth about the block similarity, we modify the *backends*

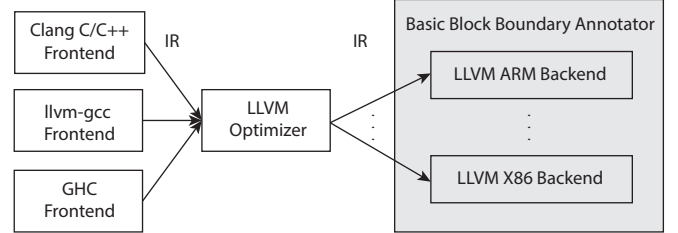


Fig. 6: LLVM architecture. The basic-block boundary annotator is added into the backends of different architectures.

of various architectures in the LLVM compiler. As shown in Figure 6, the LLVM compiler consists of various frontends (that compile source code into a uniform Intermediate Representation (IR)), the middle-end optimizer, and various architecture-dependent backends (that generate the corresponding assembly code). We modify the backends to add the basic-block boundary annotator, which not only clearly marks the boundaries of blocks, but also annotates a unique ID for each generated assembly block in a way that *all assembly blocks compiled from the same IR block (i.e., the same piece of source code), regardless of their architectures, will obtain the same ID*.

To this end, we collect various open-sourced software projects, and feed the source code into the modified LLVM compiler to generate a large number of basic blocks for different architectures. After preprocessing (Section IV-C) and data deduplication, for each basic blocks B^{x86} , one similar block B^{ARM} with the same ID is sampled to construct one training example, $\langle B^{x86}, B^{ARM}, 1 \rangle$, which is added to the dataset. By continually sampling, we can construct a large number of similar basic-block pairs.

2) *Generating Dissimilar Basic-Block Pairs*: While two basic blocks with the same ID are always semantically equivalent, two blocks with different IDs may not necessarily be dissimilar, as there can be different pieces of source code to be semantically equivalent, resulting in many equivalent basic blocks compiled from different pieces of source code.

To address this issue, we utilize n -gram to measure the text similarity between basic blocks compiled for the *same* architecture, and use the results to find dissimilar basic-block pairs across *different* architectures. Assume a block B_1^{ARM} compiled for ARM is *equivalent* to a block B_1^{x86} compiled for x86 (they have the same ID); and another block B_2^{x86} compiled for x86 is *dissimilar* to B_1^{x86} according to the n -gram similarity comparison. The two blocks, B_1^{ARM} and B_2^{x86} , are regarded as dissimilar, and a piece of labeled data $\langle B_1^{ARM}, B_2^{x86}, 0 \rangle$ is added to the dataset. Our experiments set n as 4 and the similarity threshold as 0.5; that is, if two blocks, through this procedure, have a similarity score smaller than 0.5, they are labeled as dissimilar. This way, we can obtain a large number of dissimilar basic-block pairs across different architectures.

Note that this dataset (containing labeled similar and dissimilar block pairs) is used for training and testing the basic-block embedding model, and thus the source code and basic-block boundary annotator are needed in order to establish the ground truth for the basic-block pairs. But once the model is trained and used in real application scenarios (e.g., for detecting Heartbleed vulnerability), binary executables can be directly disassembled to the assembly code for similarity detection.

VI. PATH/CODE COMPONENT SIMILARITY COMPARISON

Detection of code component similarity is an important problem. Existing work can only either work on a *single* architecture [60], [20], [37], [42], [56], [53], [27], [26], or compare *functions* of varying architectures [50], [17], [18], [66]. However, as a critical code part may be inserted inside a function to avoid detection [29], [27], [37], how to perform cross-architecture code similarity comparison *beyond function pairs* is a *new* and more challenging problem.

We propose to decompose the CFG of the query code component \mathcal{Q} into multiple paths. For each path from \mathcal{Q} , we compare it to many paths from the target program \mathcal{T} , to calculate a path similarity score by adopting the *Longest Common Subsequence* (LCS) dynamic programming algorithm with basic blocks as sequence elements. By trying more than one path, we can use the path similarity scores collectively to detect whether a component in \mathcal{T} is similar to \mathcal{Q} .

A. Path Similarity Comparison

A linearly independent path is a path that introduces at least one new node (i.e., basic block) that is not included in any previous linearly independent paths [62]. Once the starting block of \mathcal{Q} and several candidate starting blocks of \mathcal{T} are identified (presented in the next section), the next step is to explore paths to calculate a path similarity score. For \mathcal{Q} , we select a set of linearly independent paths from the starting block. We first unroll each loop in \mathcal{Q} once, and adopt the Depth First Search algorithm to find a set of linearly independent paths.

For each linearly independent path of \mathcal{Q} , we need to find the highest similarity score between the query path and the many paths of \mathcal{T} . To this end, we apply a recently proposed code similarity comparison approach, called `COP` [37] (it is powerful for handling many types of obfuscations but can only handle code components of the same architecture). `COP` combines the Longest Common Subsequent (LCS) algorithm and basic-block similarity comparison to compute the LCS of semantically equivalent basic blocks (SEBB). However, `COP`'s basic-block similarity comparison relies on symbolic execution and theorem proving, which is very computationally expensive. On the contrary, our work adopts techniques in NMT to *significantly speed up basic-block similarity comparison*, and hence is much more scalable for analyzing large codebases.

Here we briefly introduce how `COP` applies LCS to detect path similarity. It adopts breadth-first search in the *inter-procedural* CFG of the target program \mathcal{T} , combined with the LCS dynamic programming to compute the highest score of the LCS of SEBB. For each step in the breadth-first dynamic programming algorithm, the LCS is kept as the “longest path” computed so far for a block in the query path. The LCS score of the last block in the query path is the highest LCS score, and is used to compute a path similarity score. Definition 2 gives a high-level description of a path similarity score.

Definition 2: (Path Similarity Score) Given a linearly independent path \mathcal{P} from the query code component, and a target program \mathcal{T} . Let $\Gamma = \{\mathcal{P}_1^t, \dots, \mathcal{P}_n^t\}$ be all of the linearly independent paths of \mathcal{T} , and $|\text{LCS}(\mathcal{P}, \mathcal{P}_i^t)|$ be the length of the LCS of SEBB between \mathcal{P} and \mathcal{P}_i^t , $\mathcal{P}_i^t \in \Gamma$. Then, the path

similarity score for \mathcal{P} is defined as

$$\psi(\mathcal{P}, \mathcal{T}) = \frac{\max_{\mathcal{P}_i^t \in \Gamma} |\text{LCS}(\mathcal{P}, \mathcal{P}_i^t)|}{|\mathcal{P}|}$$

B. Component Similarity Comparison

Challenge. *The location that the code component gets embedded into the containing target program is unknown*, and it is possible for it to be inserted into the middle of a function. It is important to determine the correct starting points so that the path exploration is not misled to irrelevant code parts of the target program. This is a *unique challenge* compared to function-level code similarity comparison.

Idea. We look for the starting blocks in the manner as follows. First, the embeddings of all basic blocks of the target program \mathcal{T} are stored in a locality-sensitive hashing (LSH) database for efficient online search. Next, we begin with the first basic block in the query code component \mathcal{Q} as the starting block, and search in the database to find a semantically equivalent basic block (SEBB) from the target program \mathcal{T} . If we find one or several SEBBs, we proceed with the path exploration (Section VI-A) on each of them. Otherwise, we choose another block from \mathcal{Q} as the starting block [37], and repeat the process until the last block of \mathcal{Q} is checked.

Component similarity score. We select a set of linearly independent paths from \mathcal{Q} , and compute a path similarity score for each linearly independent path. Next, we assign a weight to each path similarity score according to the length of the corresponding query path. The final component similarity score is the weighted average score.

Summary. By integrating our cross-lingual basic-block embedding model with an existing approach [37], we have come up with an effective and efficient solution to cross-architecture code-component similarity comparison. Moreover, it demonstrates how the efficient, precise and scalable basic-block embedding model can benefit numerous systems [20], [37], [42] that rely on basic-block similarity comparison.

VII. EVALUATION

We empirically evaluate INNEREYE on its accuracy, efficiency, and scalability. First, we describe the experiment setup (Section VII-A) and discuss the datasets used in our evaluation (Section VII-B). Next, we examine the impact of preprocessing on out-of-vocabulary instructions (Section VII-C) and the quality of the instruction embedding model (Section VII-D). We then evaluate whether INNEREYE-BB can successfully detect the similarity of blocks compiled for different architectures (Problem I). We evaluate its accuracy and efficiency (Sections VII-E and VII-G), and discuss hyperparameter selection (Section VII-F). We also compare it with a machine learning-based basic-block comparison approach that utilizes a set of manually selected features [18], [66] (Section VII-E3). Finally, we present three real-world case studies demonstrating how INNEREYE-CC can be applied for cross-architecture code component search and cryptographic function search under realistic conditions (Problem II) in Section VII-H.

TABLE I: The number of basic-block pairs in the training, validation and testing datasets.

	Training			Validation			Testing			Total		
	Sim.	Dissim.	Total	Sim.	Dissim.	Total	Sim.	Dissim.	Total	Sim.	Dissim.	Total
O1	35,416	35,223	70,639	3,902	3,946	7,848	4,368	4,354	8,722	43,686	43,523	87,209
O2	45,461	45,278	90,739	5,013	5,069	10,082	5,608	5,590	11,198	56,082	55,937	112,019
O3	48,613	48,472	97,085	5,390	5,397	10,787	6,000	5,988	11,988	60,003	59,857	119,860
Cross-opts	34,118	33,920	68,038	3,809	3,750	7,559	4,554	4,404	8,958	42,481	42,074	84,555
Total	163,608	162,893	326,501	18,114	18,162	36,276	20,530	20,336	40,866	202,252	201,391	403,643

A. Experiment Setup

We adopt word2vec [40] to learn instruction embeddings, and implemented our cross-lingual basic-block embedding model in Python using the Keras [10] platform with TensorFlow [1] as backend. Keras provides a large number of high-level neural network APIs and can run on top of TensorFlow. Like in the work CoP [37], we require that the selected linearly independent paths cover at least 80% of the basic blocks in each query code component; the largest number of the selected linearly independent paths in our evaluation is 47. INNEREYE-CC (the LCS algorithm with path exploration) is implemented in the BAP framework [4] which constructs CFGs and call graph and builds the inter-procedural CFG. INNEREYE-CC queries the block embeddings (computed by INNEREYE-BB) stored in a LSH database. The experiments were performed on a computer running the Ubuntu 14.04 operating system with a 64-bit 2.7 GHz Intel® Core™ i7 CPU and 32 GB RAM.

B. Dataset

We first describe the dataset (**Dataset I**), as shown in Table I, used to evaluate the cross-lingual basic-block embedding model (INNEREYE-BB). All basic-block pairs in the dataset have known ground truth for metric validation. In particular, we prepare this dataset using OpenSSL (v1.1.1-pre1) and four popular Linux packages, including coreutils (v8.29), findutils (v4.6.0), diffutils (v3.6), and binutils (v2.30). We use two architectures (x86-64 and ARM) and clang (v6.0.0) with four different compiler optimization levels (O1-O3) to compile each program. In total, we obtain 437,104 basic blocks for x86, and 393,529 basic blocks for ARM.

We consider two basic blocks compiled from the same source code as similar, or dissimilar otherwise (Section V-E). Based on this, we generate 202,252 similar basic-block pairs (*one compiled from x86 and another from ARM*; as shown in the 11th column of Table I), where 43,686 pairs, 56,082 pairs, 60,003 pairs, and 42,481 pairs are compiled using O1, O2, O3, and different optimization levels, respectively. Similarly, we generate 201,391 dissimilar basic-block pairs (as shown in the 12th column of Table I), where 43,523 pairs, 55,937 pairs, 59,857 pairs, and 42,074 pairs are compiled using O1, O2, O3, and different optimization levels, respectively.

C. Evaluation on Out-Of-Vocabulary Instructions

As the pre-processing is applied to address the issue of out-of-vocabulary (OOV) instructions (Section IV-C), we evaluated its impact, and seek to understand: a) how the vocabulary size (the number of columns in the instruction embedding matrix) grows with or without pre-processing, and b) the number of OOV cases in later instruction embedding generation.

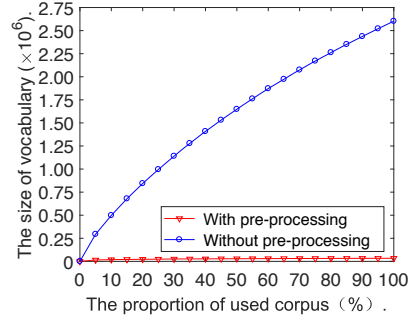


Fig. 7: The growth of vocabulary size.

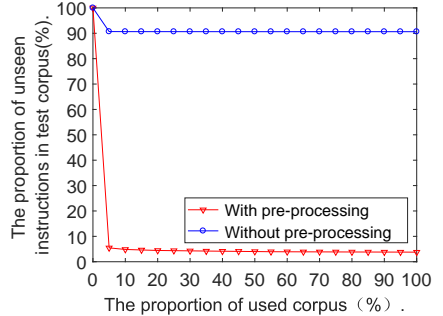


Fig. 8: The proportion of unseen instructions.

To this end, we collected various x86 binaries, and disassembled these binaries to generate a corpus which contains 6,115,665 basic blocks and 39,067,830 assembly instructions. We then divided the corpus equally into 10 parts. We counted the vocabulary size in terms of the percentage of the corpus analyzed, and show the result in Figure 7. The red line and the blue line show the growth of the vocabulary size when pre-processing was and was not applied, respectively. It can be seen that the vocabulary size grows fast and becomes uncontrollable when the corpus was not pre-processed.

We next investigated the number of OOV cases, i.e., unseen instructions, in later instruction embedding generation. We selected two binaries that never appeared in the previous corpus, which contains 67,862 blocks and 453,724 instructions. We then counted the percentage of unseen instructions that did not exist in the vocabulary, and show the result in Figure 8. The red and blue lines show the percentage of unseen instructions when the vocabulary was built with or without pre-processing, respectively. We can see that after pre-processing, only 3.7% unseen instructions happened in later instruction embedding generation; for an OOV instruction, a zero vector is assigned. This shows that the pre-processed dataset has a good coverage of the various instructions.

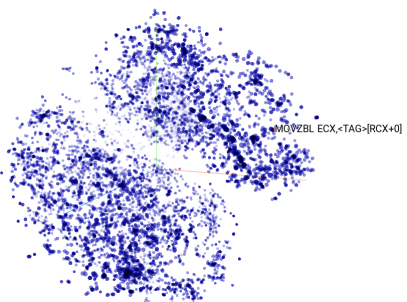


Fig. 9: Visualization of all the instructions for x86 and ARM.

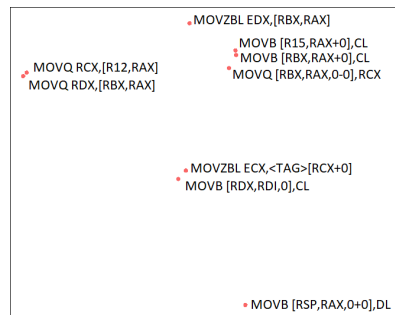


Fig. 10: Visualization of a particular x86 instruction and its neighbor instructions.

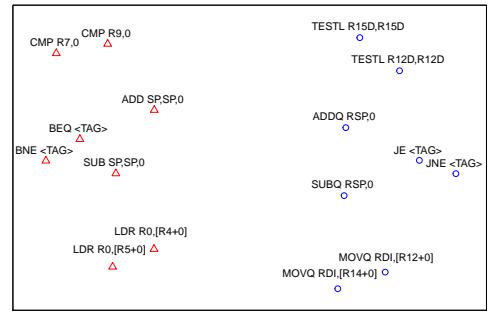


Fig. 11: Visualization of a set of instructions for x86 and ARM. The blue circle and red triangle represent an x86 instruction and an ARM instruction, respectively.

D. Qualitative Analysis of Instruction Embeddings

We present our results from qualitatively analyzing the instruction embeddings for the two architectures, x86 and ARM. We first use t-SNE [39], a useful tool for visualizing high-dimensional vectors, to plot the instruction embeddings in a three-dimensional space, as shown in Figure 9. A quick inspection immediately shows that the instructions compiled for the same architecture are group together. Thus the most significant factor that influences code is the architecture as it introduces more syntactic variations; this is the reason why cross-architecture code similarity detection is much more difficult than single-architecture code similarity detection.

We then zoom in Figure 9, and plot a particular x86 instruction `MOVZBL ECX,<TAG>[RCX+0]` and its neighbor instructions in Figure 10. It can be observed that the `mov` family instructions are close to each other.

We next randomly pick up eight x86 instructions. For each x86 instruction, we select its similar counterpart from ARM based on our prior knowledge and experience. We then plot the eight pairs of instructions in Figure 11. We use analogical reasoning techniques to find similarity of instructions. We use $[x]$ and $\{y\}$ to represent the embedding of an ARM instruction x , and an x86 instruction y , respectively; and $\cos([x_1], [x_2])$ refers to the cosine distance between two ARM instructions, x_1 and x_2 . We have the following findings: (1) $\cos(\{\text{ADD SP, SP, 0}\}, \{\text{SUB SP, SP, 0}\})$ is approximate to $\cos(\{\text{ADDQ RSP, 0}\}, \{\text{SUBQ RSP, 0}\})$. (2) $\cos(\{\text{ADD SP, SP, 0}\}, \{\text{ADDQ RSP, 0}\})$ is approximate to $\cos(\{\text{SUB SP, SP, 0}\}, \{\text{SUBQ RSP, 0}\})$. This is similar to other instruction pairs. We limit the presented examples to eight due to space limitation. In our manual investigation, we find many such semantic analogies that are automatically learned. Therefore, the analysis exhibits that the instruction embedding model learns semantic information of instructions.

E. Accuracy of INNEREYE-BB

We now evaluated the accuracy of our INNEREYE-BB. All evaluations in this subsection were conducted on Dataset I.

1) Model Training: We divide Dataset I into three parts for training, validation, and testing: for similar basic-block pairs, 80% of them are used for training, 10% for validation, and the remaining 10% for testing; the same splitting rule is applied to

the dissimilar block pairs as well. Table I shows the statistic results. In total, we have four training datasets: the first three datasets contain the basic-block pairs compiled with the same optimization level (O1, O2, and O3), and the last one contains the basic-block pairs compiled with different optimization levels (cross-opts). Note that in all the datasets, the two basic blocks of each pair are compiled for different architectures. This is the same for validation and testing datasets. In addition, during splitting, we guarantee that *the basic blocks compiled from the same source code are never split into two different subsets*. Through this, we can examine whether our model can work for unseen blocks. Note that the instruction embedding matrices for different architectures can be precomputed and reused.

We use the four training datasets to train INNEREYE-BB individually for 100 epochs. After each epoch, we measure the AUC and loss on the corresponding validation datasets, and save the models achieving the best AUC as the base models.

2) Results: We now evaluate the accuracy of the base models using the corresponding testing datasets. The red lines in the first four figures in Figure 12, from (a) to (d), are the ROC of the similarity test. As each curve is close to the left-hand border and top border, our models have good accuracy.

To further evaluate the performance of our models on basic blocks with different sizes, we created large-size and small-size testing subsets. If a basic block contains less than 5 instructions it belongs to the small-size subset; a block containing more than 20 instructions belongs to the large-size subset. We then evaluate the corresponding ROC. Figure 12e and Figure 12f show the ROC results evaluated on the large-size subset (221 pairs) and small-size subset (2409 pairs), respectively, where the basic-block pairs are compiled with the O3 optimization level. The ROC results evaluated on the basic-block pairs compiled with other optimization levels are similar, and are omitted here due to space limitation. We can observe that our models achieve good accuracy for both small blocks and large ones.

Examples. Table II shows six pairs of semantically equivalent basic blocks (after pre-processing) compiled for different architectures. It can be observed that the two blocks of each pair are very different in terms of the instruction sets, CPU registers, and memory access strategies. Our model reported each pair is similar basic-block pair (with the output label 1), and is effective in measuring basic block semantics similarity.

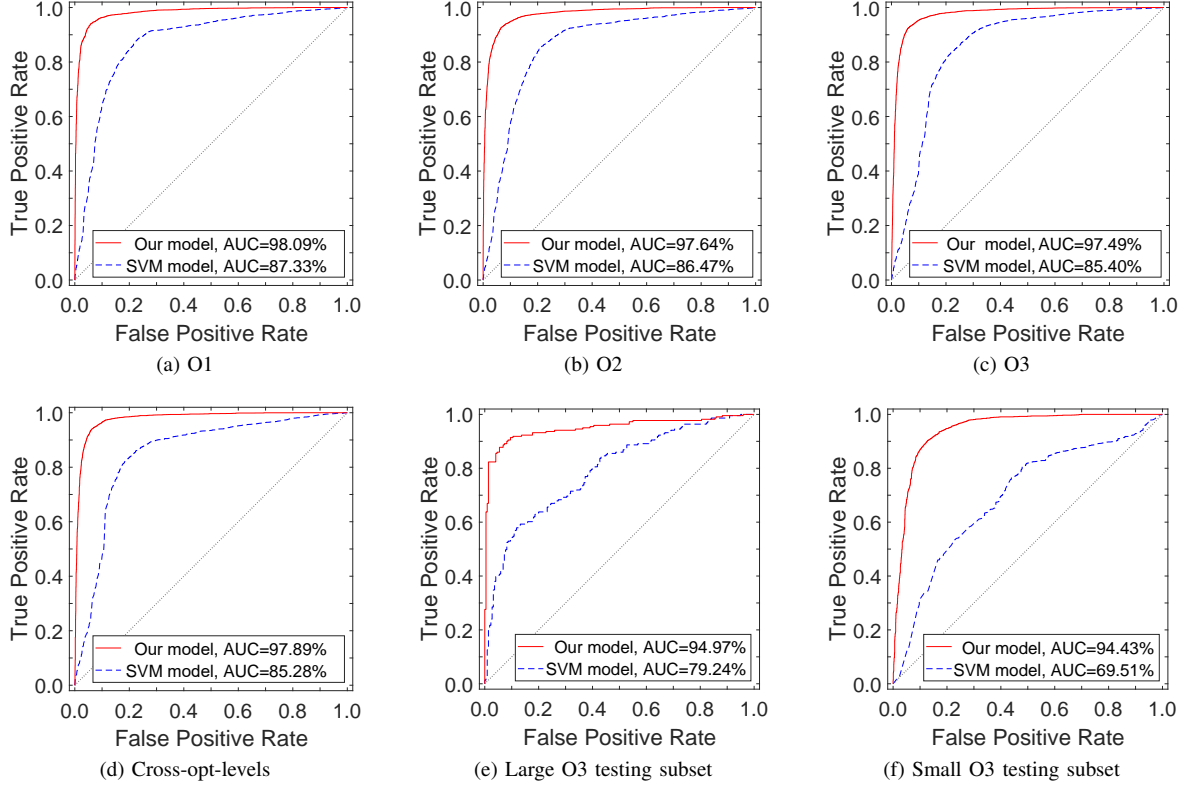


Fig. 12: The ROC results evaluated on the four testing datasets.

TABLE II: Examples of semantically equivalent basic blocks for different architectures.

Pair 1		Pair 2		Pair 3	
<i>x86</i>	<i>ARM</i>	<i>x86</i>	<i>ARM</i>	<i>x86</i>	<i>ARM</i>
CALLQ FOO	BL FOO	ANDL R12D, 0	LDR R8, [SP+0]	XORL EBX, EBX	CMP R4, 0
MOVQ [RIP+<TAG>], RAX	STR R0, [R7]	JE <TAG>	ANDS R1, R0, 0	TESTL EBP, EBP	BLT <TAG>
TESTQ RAX, RAX	CMP R0, 0	BEQ <TAG>	BEQ <TAG>	JS <TAG>	
JE <TAG>					
Pair 4		Pair 5		Pair 6	
<i>x86</i>	<i>ARM</i>	<i>x86</i>	<i>ARM</i>	<i>x86</i>	<i>ARM</i>
PUSHQ R14	PUSH {R4, R5, R11, LR}	MOVQ EAX, R13D	MOV R0, R6	MOVQ RAX, <TAG>+[RIP+0]	LDR R0, <TAG>
PUSHQ RBX	MOV R4, R0	ADDQ RSP, 0	ADD SP, SP, 0	CMPQ RAX, [RSP+0]	LDR R1, [R0+0]
PUSHQ RAX	LDR R0, [R4+0]	POPQ RBX	POP {R4,R5,R6,R7,R11,LR}	JNE <TAG>	LDR R2, [R0+0]
MOVQ RBX, RDI	LDRB R2, [R0]	POPQ R12	POPQ R13		LDR R3, [SP+0]
MOVQ RAX, [RBX+0]	CMP R2, 0	POPQ R14	POPQ R15		LDR R7, [SP+0]
CMPB [RAX], 0	BNE <TAG>	RETQ			EOR R2, R2, R7
JNE <TAG>					EOR R1, R1, R3
					ORRS R1, R1, R2
					BNE <TAG>

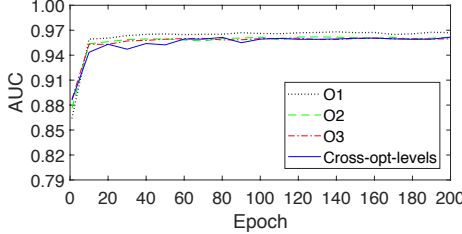
3) *Comparison with Manually Selected Features*: Several methods are proposed for cross-architecture basic block similarity detection, e.g., fuzzing [50], symbolic execution [20], [37], and basic-block feature-based machine learning classifier [18]. As fuzzing and symbolic execution are quite expensive, we compare our model against the SVM classifier that analyzes the six *manually* selected block features proposed in Gemini (see Table I in [66]).

We extracted six features (e.g., the number of instructions and constants) from each block to represent the block, and all blocks in the training dataset to train the SVM classifier. We adopted leave-one-out cross-validation with $K = 5$ and

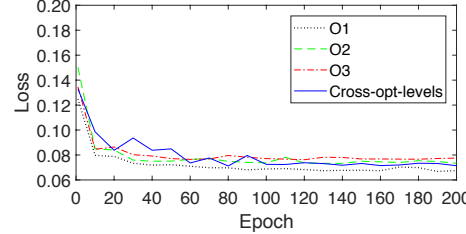
used the Euclidean distance to measure the similarity of blocks. By setting the complexity parameter $c = 1.0$, $\gamma = 1.0$ and choosing the RBF kernel, the SVM classifier achieved the best AUC value. Figure 12 shows the comparison results on different testing subsets. We can see that our models outperform the SVM classifier and achieve higher AUC values. This is because the *manually* selected features lose the semantics of the instruction sequence in a block and thus causes imprecision, and INNEREYE-BB *automatically* encodes the block semantics.

F. Hyperparameter Selection for INNEREYE-BB

We next investigate the stability of INNEREYE-BB with respect to different hyperparameters. In particular, we look into



(a) AUC vs. # of epochs.



(b) Loss vs. # of epochs.

(%)	Optimization levels			Cross -opts
	O1	O2	O3	
50	95.77	95.23	94.97	95.39
100	96.83	96.33	95.99	95.82
150	96.89	96.33	96.24	95.86

(c) AUC vs. instruction embedding dimensions.

(%)	Optimization levels			Cross -opts
	O1	O2	O3	
10	95.57	95.73	95.48	95.59
30	95.88	95.65	96.17	95.45
50	96.83	96.33	95.99	95.82

(d) AUC vs. block embedding dimensions.

(%)	Optimization levels			Cross -opts
	O1	O2	O3	
1	95.88	95.65	96.17	95.45
2	97.83	97.49	97.59	97.45
3	98.16	97.39	97.48	97.76

(e) AUC vs. # of network layers.

(%)	Optimization levels			Cross -opts
	O1	O2	O3	
LSTM	96.83	96.33	95.99	95.82
GRU	96.15	95.30	95.83	95.71
RNN	91.39	93.26	92.60	92.66

(f) AUC vs. network hidden unite types.

Fig. 13: Stability of our model with respect to different hyperparameters. Figure 13a and Figure 13b are evaluated on the validation datasets of Dataset I, and others are evaluated on the testing datasets of Dataset I.

the stability across the number of epochs, the dimensionality of the embeddings, network depth, and hidden unit types. We use the validation datasets of Dataset I to examine the impact of the number of epochs, and use the testing datasets of Dataset I to examine the impact of other hyperparameters.

1) Number of Epochs: To see whether the accuracy of the model fluctuates during training, we trained the model for 200 epochs and evaluated the model every 10 epochs for the AUC and loss. The results are displayed in Figure 13a and Figure 13b. We observe that the AUC value steadily increases and is stabilize at the end of epoch 20; and the loss value decreases quickly and almost stays stable after 20 epochs. Therefore, we conclude that the model can be quickly trained to achieve reasonably good performance.

2) Embedding Dimensions: We next measure the impact of the instruction embedding and block embedding dimensions.

Instruction embedding dimension. We varied the instruction embedding dimension, and evaluated the corresponding AUC values shown in Figure 13c. We observe that increasing the embedding dimensions yields higher performance; and the AUC values corresponding to the embedding dimension higher than 100 are close to each other. Since a higher embedding dimension leads to higher computational costs (requires longer training time), we conclude that a moderate dimension of 100 is a good trade-off between effectiveness and efficiency.

Block embedding dimension. We next varied the block embedding dimension, and evaluated the corresponding AUC values shown in Figure 13d. We observe that the performance of the models with 10, 30 and 50 block embedding dimensions are close to each other. Since a higher embedding dimension leads to higher computational costs, we conclude that a dimension of 50 for block embeddings is a good trade-off.

3) Network Depth: We changed the number of layers of each LSTM-RNN, and evaluated the corresponding AUC values. Figure 13e shows that the LSTM networks with two and three layers outperform the network with a single layer, and the AUC values for the networks with two and three layers are close to each other. Because adding more layers increases

TABLE III: Training time of the instruction embedding model with respect to different embedding dimensions.

Instruction embedding dimension	50	100	150
Training time (second)	82.71	84.22	89.75

the computational complexity and does not help much on the performance, we choose the network depth as 2.

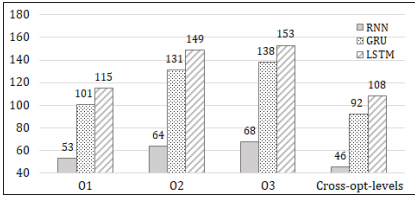
4) Network Hidden Unit Types: LSTM is a specific RNN, developed to address the difficulty of capturing long term memory in the basic RNN. Another variant, called GRU, is simpler than LSTM and has become increasingly popular. We conducted experiments on comparing these three types of network unit. Figure 13f shows the comparison results. It can be seen that LSTM and GRU are more powerful than the basic RNN, and LSTM shows the highest AUC values.

G. Efficiency of INNEREYE-BB

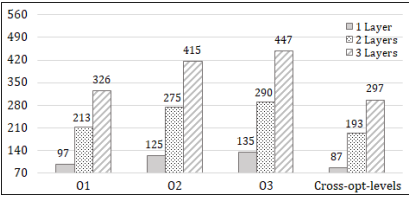
1) Training Time: We first analyzed the training time for both the instruction and basic-block embedding models.

Instruction embedding model training time. The training time is linear to the number of epochs and the corpus size. We use Dataset I, containing 437,104 blocks for x86 and 393,529 blocks for ARM, with 6,199,651 instructions in total, as the corpus to train the instruction embedding model. The corpus contains 49,760 distinct instructions which form a vocabulary. We used 10^{-5} as down sampling rate and set the parameter `mini-word-count` as zero (no word is ignored during training), and trained the model for 100 epochs. Table III shows the training time with respect to different instruction embedding dimensions. We can see that the instruction embedding model can be trained in a very short period of time.

Block embedding model training time. We next evaluate the time used for training the basic-block embedding model. The training time is linear to the number of epochs and the number of training samples. The results are showed in Figure 14. The number above each bar is the time (*second per epoch*) used



(a) Training time of single-layer networks with respect to different hidden unit types.



(b) Training time of LSTM-RNNs with respect to different number of network layers

Fig. 14: Training time of the basic-block embedding model. The instruction embedding dimension is 100, and the block embedding dimension is 50. The number above each bar is the time (*second per epoch*) used to train the model.

to train the model. Figure 14a shows the training time with respect to different types of network hidden unit. Figure 14b displays the training time of the LSTM networks in terms of different number of network layers. In general, LSTM takes longer training time, and a more complicated model (with more layers) requires more time per epoch.

Earlier we have shown that the block embedding model with 2 network layers and 20 epochs of training can achieve a pretty good performance (Section VII-F), which means that it requires five and a half hours ($=(213 + 275 + 290 + 193) \times 20/3600$) to train the four models on the four training subsets, and each model takes around an hour and a half for training. With a single network layer, each model only needs about 40 mins for training and can still achieve a good performance.

2) Testing Time: We next investigate the testing time of INNEREYE-BB. We are interested in the impacts of the number of network layers and the dimension of block embeddings, in particular. Table 15 summaries the similarity test on the four testing datasets in Dataset I. The result indicates that the number of network layers is the major contributing factor of the computation time. Take the second column as an example. For a single-layer LSTM network with the block embedding dimension as 50, it takes 0.41 ms ($= 3.530/8722$) in average to measure the similarity of two blocks, while a double-layer LSTM network requires 0.76 ms ($= 6.663/8722$) in average.

Comparison with Symbolic Execution. We appreciate the authors [37] who share with us their basic-block similarity comparison tool that relies on symbolic execution and theorem proving. We compared our embedding model to the symbolic execution-based tool. We randomly selected 1,000 block pairs and used the symbolic execution-based tool to measure the detection time for each pair. The result shows that the INNEREYE-BB runs 3700x to 140000x faster, and the speedup can be as high as 8000x on average.

The reason for the high efficiency of our model is that most computations of INNEREYE-BB are implemented as easy-to-compute matrix operations (e.g., matrix multiplication, matrix summation, and element-wise operations over a matrix). Moreover, such operations can be parallelized to utilize multi-core CPUs to achieve further speedup.

H. Code Component Similarity Comparison

We conduct three case studies to demonstrate how INNEREYE-CC can handle real-world programs for *cross-architecture code component similarity detection*.

(Second)	Optimization levels			Cross -opts
	O1	O2	O3	
L=1, D=30	3.040	3.899	4.137	2.944
L=1, D=50	3.530	4.702	4.901	3.487
L=2, D=30	6.359	8.237	8.780	6.266
L=2, D=50	6.663	8.722	9.139	6.625

Fig. 15: Testing time of INNEREYE-BB with respect to different number of network layers and block embedding dimensions. The instruction embedding dimension is 100. L denotes the number of network layers. D denotes the block embedding dimension.

1) `thttpd`: This experiment evaluated `thttpd` (v2.25b) and `stthttpd` (v2.26.4), where `stthttpd` is forked from `thttpd` for maintenance. Thus, their codebases are similar, with many patches and new building systems added to `stthttpd`. To measure false positives, we tested our tool on four independent programs, including `thttpd` (v2.25b), `atphttpd` (v0.4b), `boa` (v0.94.13), and `lighttpd` (v1.4.30). We used two architectures (x86 and ARM) and `clang` with different compiler optimization levels (O1–O3) to compile each program.

We considered a part of the `httpd_parse_request` function as well as the functions invoked within this code part from `thttpd` as the query code component, and checked whether it is reused in `stthttpd`. Such code part checks for HTTP/1.1 absolute URL and is considered as critical. We first identified the starting blocks both in the query code component and the target program `stthttpd` (Section VI-B), and proceed with the path exploration to calculate the similarity score, which is 91%, indicating that `stthttpd` reuses the query code component. The whole process was finished within 2 seconds. However, `CoP` [37] (it uses symbolic execution and theorem proving to measure the block similarity) takes almost one hour to complete. Thus, by adopting techniques in NMT to speed up block comparison, INNEREYE is more efficient and scalable.

To measure false positives, we tested INNEREYE against four independently developed programs. We used the query code component to search for the similar code components in `atphttpd` (v0.4b), `boa` (v0.94.13), and `lighttpd` (v1.4.30). Very low similarity scores (below 4%) were reported.

2) Cryptographic Function Detection: We next applied INNEREYE to the cryptographic function detection task. We chose MD5 and AES as the query cryptographic functions, and searched for their implementations in 13 target programs ranging from small to large real-world software, including `cryptlib` (v3.4.2), `OpenSSL` (v1.0.1f), `openssh` (v6.5p1), `git` (v1.9.0), `libgcrypt` (v1.6.1), `truecrypt` (v7.1a), `berkeley DB` (v6.0.30), `MySQL` (v5.6.17), `glibc` (v2.19), `p7zip` (v9.20.1), `cmake` (v2.8.12.2), `thttpd` (v2.25b), and `stthttpd` (v2.26.4). We used x86 and ARM, and `clang` with O1–O3 optimization levels to compile each program.

MD5. MD5 is a cryptographic hash function that produces a 128-bit hash value. We first extracted the implementation of MD5 from `OpenSSL` compiled for x86 with `-O2`. The functionality of MD5 include initializing hash digests, compressing messages, and updating hash digests. A part of the MD5 code that implements message compressing is selected as the query.

We used the query code component to search for the similar code components from the target programs. The results show that `cryptlib`, `openssh`, `libgcrypt`, `MySQL`, `glibc`, and `cmake` implement MD5 with the similarity scores between 88% and 93%. We checked the source code and confirmed it.

AES. AES is a 16-byte block cipher and processes input via a substitution-permutation network. We extracted the implementation of AES from OpenSSL compiled for ARM with `-O2`, and selected a part of the AES code that implements transformation iterations as the query code component.

We tested the query code component to check whether it is reused in the target programs, and found that `cryptlib`, `openssh`, `libgcrypt`, `truecrypt`, `berkeley DB`, and `MySQL` contain AES with the similarity scores between 86% and 94%, and the others do not. We checked the source code and obtained consistent results.

The case studies demonstrate that INNEREYE-CC is an effective and precise tool for cross-architecture binary code component similarity detection.

VIII. DISCUSSION

Based on the insight that binaries compiled for different architectures are expressed in different (assembly) languages, we propose the neural network-based cross-lingual basic-block embedding model by leveraging the ideas and techniques of NMT. Our system is able to (a) directly work on binary code, (b) analyze code of *different architectures*, (c) measure code similarity *beyond function pairs*, and (d) compare code similarity efficiently. Previous works are largely unable to meet all these requirements. Moreover, many prior systems built on basic block comparison or representation [20], [42], [37], [50], [18] can benefit from our block embedding model, which provides more precise and efficient basic block comparison and information extraction.

Gemini [66] also applies neural networks to code similarity comparison. There are two main differences between our systems and theirs. First, Gemini uses *manually* selected features (such as the number of instructions and constants) to represent a basic block, while our block embedding model, INNEREYE-BB, *automatically* selects useful features and uses the block embeddings (Section V) to represent basic blocks. As shown in our evaluation (Section VII-D), the manually selected features cannot capture the semantics information of the instruction sequence within a block, and the precision of INNEREYE-BB outperforms it by a large margin.

Second, Gemini adopts structure2vec to embed the *whole* graph (i.e., CFG) of a function into an embedding and uses the distance of the embeddings to measure function code similarity. Hence, Gemini only works on the *function-level*. In contrast, INNEREYE-CC is capable of detecting code similarity without being limited to function pair comparison.

Limitations. First, our approach relies on the quality of basic block extraction. Although LLVM provides reasonable accuracy in our evaluation, we can use more advanced techniques such as [3], [54] to further improve accuracy.

Second, we evaluated our tool on its tolerability of the syntactic variations introduced by different architectures and

compiling setup; but we do not evaluate the impact of code obfuscation. If provided with enough training examples of obfuscated binary basic blocks, we expect that our model can still be trained to capture the intrinsic characteristics of these binary basic blocks. Since our main focus in this paper is to propose *cross-architecture* code similarity comparison *beyond function pairs* and fill the current gap in binary code analysis, we leave the evaluation for this case to future work.

IX. CONCLUSION

Inspired by Neural Machine Translation, which is able to compare the meanings of sentences of different languages, we propose a novel neural network-based basic-block similarity comparison tool INNEREYE-BB by regarding instructions as words and basic block as sentences. It is the first tool of this kind that achieves both efficiency and accuracy for cross-architecture basic-block comparison; plus, it does not rely on any manually selected features. By leveraging INNEREYE-BB, we propose the first tool INNEREYE-CC that can handle cross-architecture code similarity comparison beyond function pair. We have implemented the system and performed a comprehensive evaluation. The trained NN model, datasets, and the evaluation results are publicly available. This research has successfully demonstrated that it is promising to approach binary analysis from the angle of language processing by adapting methodologies, ideas and techniques in NLP.

REFERENCES

- [1] M. Abadi, P. Barham, J. Chen, Z. Chen, A. Davis, J. Dean, M. Devin, S. Ghemawat, G. Irving, M. Isard *et al.*, “Tensorflow: A system for large-scale machine learning,” in *OSDI*, vol. 16, 2016, pp. 265–283.
- [2] B. S. Baker, “On finding duplication and near-duplication in large software systems,” in *Reverse Engineering, 1995, Proceedings of 2nd Working Conference on*. IEEE, 1995, pp. 86–95.
- [3] T. Bao, J. Burkett, M. Woo, R. Turner, and D. Brumley, “Byteweight: Learning to recognize functions in binary code.” USENIX, 2014.
- [4] BAP: The Next-Generation Binary Analysis Platform, “<http://bap.ece.cmu.edu/>,” 2013.
- [5] Y. Bengio, R. Ducharme, P. Vincent, and C. Jauvin, “A neural probabilistic language model,” *Journal of machine learning research*, vol. 3, no. Feb, pp. 1137–1155, 2003.
- [6] M. Bilenko and R. J. Mooney, “Adaptive duplicate detection using learnable string similarity measures,” in *KDD*. ACM, 2003, pp. 39–48.
- [7] J. Bromley, I. Guyon, Y. LeCun, E. Säckinger, and R. Shah, “Signature verification using a “siamese” time delay neural network,” in *Advances in Neural Information Processing Systems*, 1994, pp. 737–744.
- [8] D.-K. Chae, S.-W. Kim, J. Ha, S.-C. Lee, and G. Woo, “Software plagiarism detection via the static api call frequency birthmark,” in *Proceedings of the 28th Annual ACM Symposium on Applied Computing*. ACM, 2013, pp. 1639–1643.
- [9] M. Chandramohan, Y. Xue, Z. Xu, Y. Liu, C. Y. Cho, and H. B. K. Tan, “Bingo: Cross-architecture cross-os binary search,” in *FSE*. ACM, 2016, pp. 678–689.
- [10] F. Chollet *et al.*, “Keras,” <https://keras.io>, 2015.
- [11] S. Chopra, R. Hadsell, and Y. LeCun, “Learning a similarity metric discriminatively, with application to face verification,” in *CVPR*, vol. 1. IEEE, 2005, pp. 539–546.
- [12] Z. L. Chua, S. Shen, P. Saxena, and Z. Liang, “Neural nets can learn function type signatures from binaries,” in *Proceedings of the 26th USENIX Conference on Security Symposium, Security*, vol. 17, 2017.
- [13] J. Chung, C. Gulcehre, K. Cho, and Y. Bengio, “Empirical evaluation of gated recurrent neural networks on sequence modeling,” *NIPS Deep Learning Workshop*, 2014.

[14] R. Collobert and J. Weston, "A unified architecture for natural language processing: Deep neural networks with multitask learning," in *Proceedings of the international conference on Machine learning*, 2008.

[15] J. Crussell, C. Gibler, and H. Chen, "Attack of the clones: Detecting cloned applications on android markets," in *European Symposium on Research in Computer Security*. Springer, 2012, pp. 37–54.

[16] S. Deerwester, S. T. Dumais, G. W. Furnas, T. K. Landauer, and R. Harshman, "Indexing by latent semantic analysis," *Journal of the American society for information science*, vol. 41, no. 6, p. 391, 1990.

[17] S. Eschweiler, K. Yakdan, and E. Gerhards-Padilla, "discovRE: Efficient cross-architecture identification of bugs in binary code." in *NDSS*, 2016.

[18] Q. Feng, R. Zhou, C. Xu, Y. Cheng, B. Testa, and H. Yin, "Scalable graph-based bug search for firmware images," in *CCS*, 2016.

[19] M. Gabel, L. Jiang, and Z. Su, "Scalable detection of semantic clones," in *ICSE*, 2008.

[20] D. Gao, M. Reiter, and D. Song, "Binhunt: Automatically finding semantic differences in binary programs," *Information and Communications Security*, pp. 238–255, 2008.

[21] Gartner says 8.4 billion connected "Things" will be in use in 2017, "<http://www.gartner.com/newsroom/id/3598917>," 2017.

[22] Z. Han, X. Li, Z. Xing, H. Liu, and Z. Feng, "Learning to predict severity of software vulnerability using only vulnerability description," in *ICSME*. IEEE, 2017, pp. 125–136.

[23] S. Hochreiter and J. Schmidhuber, "Long short-term memory," *Neural computation*, vol. 9, no. 8, pp. 1735–1780, 1997.

[24] X. Huo and M. Li, "Enhancing the unified features to locate buggy files by exploiting the sequential nature of source code," in *Proceedings of the 26th International Joint Conference on Artificial Intelligence*. AAAI Press, 2017, pp. 1909–1915.

[25] X. Huo, M. Li, and Z.-H. Zhou, "Learning unified features from natural and programming languages for locating buggy source code." in *IJCAI*, 2016, pp. 1606–1612.

[26] Y.-C. Jhi, X. Jia, X. Wang, S. Zhu, P. Liu, and D. Wu, "Program characterization using runtime values and its application to software plagiarism detection," *IEEE Transactions on Software Engineering*, 2015.

[27] Y.-C. Jhi, X. Wang, X. Jia, S. Zhu, P. Liu, and D. Wu, "Value-based program characterization and its application to software plagiarism detection," in *Software Engineering (ICSE), 2011 33rd International Conference on*. IEEE, 2011, pp. 756–765.

[28] J.-H. Ji, G. Woo, and H.-G. Cho, "A source code linearization technique for detecting plagiarized programs," in *ACM SIGCSE Bulletin*, 2007.

[29] L. Jiang, G. Mischerghi, Z. Su, and S. Glondu, "Deckard: Scalable and accurate tree-based detection of code clones," in *ICSE*, 2007.

[30] N. Kalchbrenner and P. Blunsom, "Recurrent continuous translation models." in *EMNLP*, vol. 3, no. 39, 2013, p. 413.

[31] N. Kalchbrenner, E. Grefenstette, and P. Blunsom, "A convolutional neural network for modelling sentences," in *CIKM*, 2013.

[32] T. Kamiya, S. Kusumoto, and K. Inoue, "Ccfinder: a multilingual token-based code clone detection system for large scale source code," *IEEE Transactions on Software Engineering*, 2002.

[33] R. Koschke, R. Falke, and P. Frenzel, "Clone detection using abstract syntax suffix trees," in *Reverse Engineering, 2006. WCRE'06. 13th Working Conference on*. IEEE, 2006, pp. 253–262.

[34] Y. J. Lee, S.-H. Choi, C. Kim, S.-H. Lim, and K.-W. Park, "Learning binary code with deep learning to detect software weakness," 2017.

[35] J. Li and M. D. Ernst, "CBCD: Cloned buggy code detector," in *ICSE*. IEEE, 2012, pp. 310–320.

[36] C. Liu, C. Chen, J. Han, and P. S. Yu, "Gplag: detection of software plagiarism by program dependence graph analysis," in *Proceedings of the 12th ACM SIGKDD international conference on Knowledge discovery and data mining*. ACM, 2006, pp. 872–881.

[37] L. Luo, J. Ming, D. Wu, P. Liu, and S. Zhu, "Semantics-based obfuscation-resilient binary code similarity comparison with applications to software plagiarism detection," in *FSE*. ACM, 2014.

[38] L. Luo and Q. Zeng, "Solminer: mining distinct solutions in programs," in *Proceedings of the 38th International Conference on Software Engineering Companion*. ACM, 2016, pp. 481–490.

[39] L. v. d. Maaten and G. Hinton, "Visualizing data using t-sne," *Journal of Machine Learning Research*, vol. 9, no. Nov, pp. 2579–2605, 2008.

[40] T. Mikolov, K. Chen, G. Corrado, and J. Dean, "Efficient estimation of word representations in vector space," in *Proceedings of Workshop at ICLR*, 2013.

[41] T. Mikolov, I. Sutskever, K. Chen, G. S. Corrado, and J. Dean, "Distributed representations of words and phrases and their compositionality," in *Advances in neural information processing systems*, 2013.

[42] J. Ming, M. Pan, and D. Gao, "iBinHunt: Binary hunting with interprocedural control flow," in *Proc. of the 15th Annual Int'l Conf. on Information Security and Cryptology (ICISC)*, 2012.

[43] J. Ming, F. Zhang, D. Wu, P. Liu, and S. Zhu, "Deviation-based obfuscation-resilient program equivalence checking with application to software plagiarism detection," *IEEE Transactions on Reliability*, 2016.

[44] S. A. Mokhov, J. Paquet, and M. Debbabi, "The use of nlp techniques in static code analysis to detect weaknesses and vulnerabilities," in *Canadian Conference on Artificial Intelligence*. Springer, 2014.

[45] L. Mou, G. Li, L. Zhang, T. Wang, and Z. Jin, "Convolutional neural networks over tree structures for programming language processing." in *AAAI*, vol. 2, no. 3, 2016, p. 4.

[46] J. Mueller and A. Thyagarajan, "Siamese recurrent architectures for learning sentence similarity," in *AAAI*, 2016, pp. 2786–2792.

[47] T. D. Nguyen, A. T. Nguyen, H. D. Phan, and T. N. Nguyen, "Exploring api embedding for api usages and applications," in *ICSE*. IEEE, 2017.

[48] H. Palangi, L. Deng, Y. Shen, J. Gao, X. He, J. Chen, X. Song, and R. Ward, "Deep sentence embedding using long short-term memory networks: Analysis and application to information retrieval," *IEEE/ACM Transactions on Audio, Speech and Language Processing (TASLP)*, 2016.

[49] H. Park, S. Choi, H.-i. Lim, and T. Han, "Detecting code theft via a static instruction trace birthmark for java methods," in *Industrial Informatics, 2008. INDIN 2008. 6th IEEE International Conference on*. IEEE, 2008.

[50] J. Pewny, B. Garmann, R. Gawlik, C. Rossow, and T. Holz, "Cross-architecture bug search in binary executables," in *Security and Privacy (SP), 2015 IEEE Symposium on*. IEEE, 2015, pp. 709–724.

[51] L. Prechelt, G. Malpohl, and M. Phillipssen, "Jplag: Finding plagiarisms among a set of programs," *University Karlsruhe*, 2000.

[52] S. Schleimer, D. S. Wilkerson, and A. Aiken, "Winnowing: local algorithms for document fingerprinting," in *Proceedings of the ACM SIGMOD international conference on Management of data*, 2003.

[53] D. Schuler, V. Dallmeier, and C. Lindig, "A dynamic birthmark for java," in *ASE*, 2007.

[54] E. C. R. Shin, D. Song, and R. Moazzezi, "Recognizing functions in binaries with neural networks." in *USENIX Security Symposium*, 2015.

[55] I. Sutskever, O. Vinyals, and Q. V. Le, "Sequence to sequence learning with neural networks," in *Advances in neural information processing systems*, 2014, pp. 3104–3112.

[56] H. Tamada, K. Okamoto, M. Nakamura, A. Monden, and K.-i. Matsumoto, "Dynamic software birthmarks to detect the theft of windows applications," in *International Symposium on Future Software Technology*, vol. 20, no. 22, 2004.

[57] —, "Design and evaluation of dynamic software birthmarks based on API calls," *Info. Science Technical Report NAIST-IS-TR2007011*, 2007.

[58] Z. Tian, Q. Zheng, T. Liu, and M. Fan, "DKISB: Dynamic key instruction sequence birthmark for software plagiarism detection," in *HPCC_EUC*, 2013.

[59] N. Truong, P. Roe, and P. Bancroft, "Static analysis of students' java programs," in *Proceedings of the Sixth Australasian Conference on Computing Education-Volume 30*, 2004.

[60] X. Wang, Y.-C. Jhi, S. Zhu, and P. Liu, "Behavior based software theft detection," in *CCS*. ACM, 2009.

[61] —, "Detecting software theft via system call based birthmarks," in *Computer Security Applications Conference, 2009. ACSAC'09. Annual*. IEEE, 2009, pp. 149–158.

[62] A. H. Watson and T. J. McCabe, "Structured testing: A testing methodology using the cyclomatic complexity metric," *NIST Special Publication 500-235*, 1996.

[63] M. White, M. Tufano, M. Martinez, M. Monperrus, and D. Poshyvanyk, "Sorting and transforming program repair ingredients via deep learning code similarities," *arXiv preprint arXiv:1707.04742*, 2017.

- [64] J. Wieting, M. Bansal, K. Gimpel, and K. Livescu, “Towards universal paraphrastic sentence embeddings,” *arXiv preprint:1511.08198*, 2015.
- [65] Y. Wu, M. Schuster, Z. Chen, Q. V. Le, M. Norouzi, W. Macherey, M. Krikun, Y. Cao, Q. Gao, K. Macherey *et al.*, “Google’s neural machine translation system: Bridging the gap between human and machine translation,” *arXiv preprint arXiv:1609.08144*, 2016.
- [66] X. Xu, C. Liu, Q. Feng, H. Yin, L. Song, and D. Song, “Neural network-based graph embedding for cross-platform binary code similarity detection,” in *CCS*, 2017.
- [67] W. Yang, “Identifying syntactic differences between two programs,” *Software: Practice and Experience*, vol. 21, no. 7, pp. 739–755, 1991.
- [68] F. Zhang, D. Wu, P. Liu, and S. Zhu, “Program logic based software plagiarism detection,” in *ISSRE*, 2014.